Arch. Metall. Mater. **63** (2018), 2, 681-687

DOI: 10.24425/122394

R. BĘCZKOWSKI*[#]

INFLUENCE OF CLADDING PARAMETERS WITH FCAW ON BEAD GEOMETRY WITH PLACKETT-BURMAN EXPERIMENT USED

The paper analyzes, from the geometrical aspect, the quality of the new flux cored wire intended for cladding process in function of changes in cladding parameters such as welding speed, coefficient of thermal conductivity, power source setting, the length of projecting portion of the electrode.

The results of bead geometry analysis allows to illustrate the nature of the impact of the examined input variables on parameters of generated surface. The most important parameters here are the depth of penetration and the height of clad.

The experimental data were processed using the Plackett-Burman experiment, which describes the impact of technological parameters on the main parameters used during production of resisting panels. It shows mathematical relations describing correlations between the input parameters and the value of depth of penetration and hight of bead made by Flux Cored Arc Welding (FCAW).

Keywords: cladding, hardface plate, geometry, Plackett-Burman design, FCAW

1. Introduction

A wide variety of commercial materials are available for production of special bimetal plates with high abrasive resistance. Chromium cored wires belong to welding materials that are often used to deposit cladding with high resisting. The problem to solve in industrial practice is the correct setting of the flux-cored self-shielding arc welding parameters and their impact on the final desired surface parameters [1-3].

The use of core wire in the production of clad with different chemical composition and good quality has a great potential. The problem is to determine which of the surfacing parameters have a significant impact on the final characteristics of clad. The application of Plackett-Burman design allowed to evaluate statistically the significance impact of selected parameters on the resulting geometrical parameters of the bead.

Hight of bead is one of the most important parameters of abrasion plates. The producer allows possibility to chose plate in the configuration for example 5+5. The first number gives the information about the thickness of the parent materials. Mostly S235 material grade is used. And the second number describes the thickness of hard surface. This number gives the information about the length of the lifespan. The most often plate 10+5 is used. The depth of penetration is responsible for durability and adhesive [1-12].

The development of new materials as cored wire and technologies as flux cored arc welding in the process leads to improvement of tribological properties of deposited coatings designed for protection against wear. From economic point of view using materials of the best functional properties lengthens the lifespan of the machine parts surfaces.

A convenient economical solution is making functional surfaces using hardfacing technology.

A wide variety of commercial materials are available for production of special plates with high abrasive resistance. High chromium cored wires belong to cladding materials that are often used to deposit surface with high hardness.

Advanced hardfacing alloys of high-chromium white irons deposited using cladding are well known for their wear resistance. These materials are applied in conditions requiring wear resistance.

High-chromium white irons are commonly used for the slide plate in the coal, glass and cement industry. Hardfacing alloys consist of Cr_7C_3, $Cr_{23}C_6$, Cr_3C primary and eutectic carbides and eutectic austenite or martensite. To make hardfacing layers many cladding technologies were used. Using the cored wire gives additional possibility to change the properties of clads.

In wire core different type of carbides like tungsten, vanadium, niobium, titanium, siliconium and alumina oxide with hardness to 2800 HV can be found.

Using the FCAW against wear is one of the most common technology to develop the layer over 2 mm thickness on the parent material [2-8,13-21].

* CZESTOCHOWA UNIVERSITY OF TECHNOLOGY, INSTYTUTE OF MECHANICAL TECHNOLOGIES, 21 ARMII KRAJOWEJ AV., 42-201 CZĘSTOCHOWA, POLAND,

Corresponding author: rbeczkowski@spaw.pcz.pl

2. Experiment and results

The Plackett-Burman Programme

The Plackett-Burman Programme has been established on the basis of the Hadamard matrix (designation: H), which are square matrices of order n fulfilling the equality:

$$H^T H = nE_n \tag{1}$$

whereby: E_n – the identity matrix of the order n, H^T – transposition of matrices H.

The Plackett-Burman plan is constructed on the Hadamard matrix. Values x_i – They may contain dummy variables, and their position is determined at random based on random number tables.

The program table of the Plackett-Burman plan is presented below.

N	x_1	x_2	x_3	x_4	x_5	x_6	x_7	y_i
1	+	–	–	+	–	+	+	y_1
2	+	+	–	–	+	–	+	y_2
3	+	+	+	–	–	+	–	y_3
4	–	+	+	+	–	–	+	y_4
5	+	–	+	+	+	–	–	y_5
6	–	+	–	+	+	+	–	y_6
7	–	–	+	–	+	+	+	y_7
8	–	–	–	+	–	+	+	y_8
9	0	0	0	0	0	0	0	y_9

Factors are calculated from the program table: B_i, a_i according to formulas (2) and (3):

$$Bi = \frac{\sum_{j=1}^{N} x_{ij} y_j}{\frac{N}{2}} \tag{2}$$

$$a_i = \frac{B_i}{2} \tag{3}$$

whereby: i – variable number, j – experiment number, x_{ij} – value i- this variable encoded in j-of this experiment (can assume values +1 or –1 according to the encoded test program), y_j – the value of the resulting factor j-of this experiment, N – experimental value.

Then, using dummy variables (f) in the program (for the program presented, assumed $f = 3$) for the analyzed factors, real variables (S) (e.g.: $S = 4$ was established for the given program) calculated error variance of the experiment S_n^2:

$$S_n^{\,2} = \frac{4f(a_1^{\,2} + a_2^{\,2} + \ldots + a_{N-1}^{\,2})}{4f - S - 1} \tag{4}$$

whereby: a_i, ..., a_{N-1} – the coefficients for the variables introduced.

After determining the S_n value the standard deviation S_i^2 of coefficient a_i was calculated, determined the expression:

$$S_i^{\,2} = \frac{S_n^{\,2}}{4f} \tag{5}$$

After determining the variance, the relevance of the impact of input variables to the resulting factor according to formula (6) was examined. If this condition is fulfilled, it is an important analyzed factor.

$$|a_i| \geq t_{\alpha,n} S_i \tag{6}$$

whereby: $t_{\alpha,n}$ – he critical value of t-test for significance level α and the number of degrees of freedom $n = 4f - S - 1$, S_i – standard deviation of the coefficient a_i [8-12].

Statistical inference

On the basis of characteristics of the population $–x$ determined by the same amount for different methods or wires the comparisons of characteristics of $x1$, $x2$ can be done allowing the populations studied to determine whether the differences are significant.

Test for two means implies that the populations have normal distributions $N_1(m_1,s_1)$, $N_2(m_2,s_2)$ and $s_1 = s_2$. On the basis of the numerical test, respectively n_1 and n_2, the hypothesis H_0; $m_1 = m_2$, to the alternative H_1; $m_1 \neq m_2$ is verified, it is necessary to calculate: average value $\overline{x_1}$ i $\overline{x_2}$ (7), variances $\overline{S_1^2}$ i $\overline{S_2^2}$ (8), followed by the distribution value t-Student (9) [8-12].

$$\overline{x} = \frac{1}{n} \sum_{i=1}^{n} x_i \tag{7}$$

$$S^2 = \frac{1}{n} \sum (\overline{x} - x_i)^2 \tag{8}$$

$$t = \frac{\overline{x_1} - \overline{x_2}}{\sqrt{\frac{n_1 S_1^2 + n_2 S_2^2}{n_1 + n_2 - 2} \left(\frac{1}{n_1} - \frac{1}{n_2} \right)}} \tag{9}$$

The test procedure and results

A machine with a water-cooled table was used in the sample welding and additionally the pad receiving heat from the space surfacing made of steel, aluminium and copper was laid. As the parent material S235JR steel with a thickness of 10 mm and dimensions of 200×400 mm was used, Corodur 61 (C = 5,4%, Cr = 29%, Si = 1,2%, Nb = 3,0%, Mn = 0,4%) wire was used for the cladding. The view of the work table is shown in Figure 1.

The first stage of the paper define the collections of the factors examined, fixed, distort and outputs. After exploratory studies, a set of factors that may have a significant impact on the resulting factors was identified.

The set of input factors $X_i = (x_1, x_2, x_3, x_4)$:

$x_1 = V_{NAP}$ – cladding speed, mm/min,

$x_2 = \lambda$ – coefficient of thermal conductivity, W/mK,

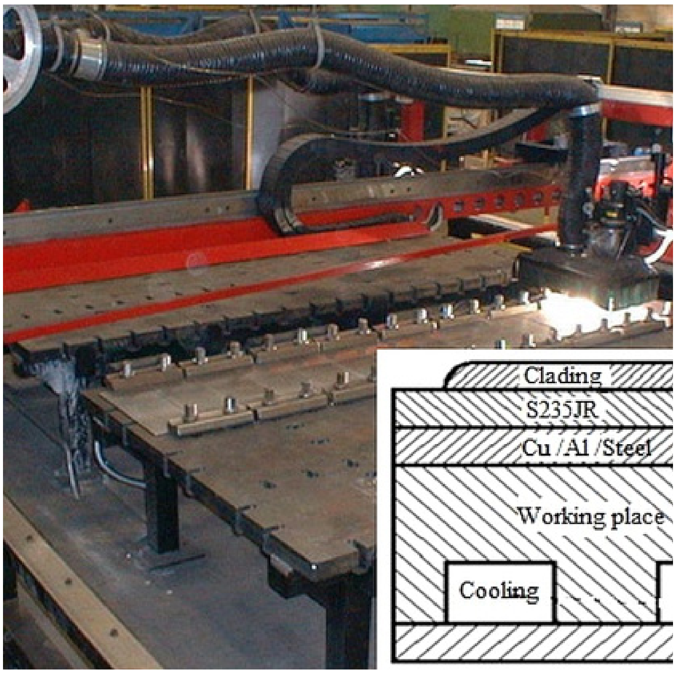

Fig. 1. The view position for the automatic welding and schematic view of the work table

$x_3 = P$ – power source setting, W,
$x_4 = L_e$ – the length the projecting portion of the electrode, mm.

The set of fixed factors $C_i = (c_1, c_2, ..., c_n)$ for: c_1 – machine, c_2 – power source, c_3 – control system, c_4 – table with cooling system, c_5 – the base material, c_6 – the number of stitches $i = 1$, c_7 – diameter of cored wire $\varphi_{dr} = 2{,}8$ mm, c_8 – type of cooling table, c_9 – ambient and material temperature $t_{ot} = 10°C$, c_{10} – width of rivets, c_{11} – oscillation speed $V_{osc} = 0{,}24$ m/min, c_{12} – wire feed speed $V_d = 5{,}8$ m/min.

The set of output factors $Y_i = (y_1, y_2:)$; $y_1 = Hn$ – hight of bead, mm; $y_1 = Hw$ – depth of penetration, mm.

To determine the range of variability of input factors $[x_{\min}, x_{\max}]$ Chebyshev polynomial was used. Degree of polynomial adopted $s = 1$, for which the minimum number of plan layouts is determined by the formula $n = s + 1$ and in the presented case it is 2.

Symbol $\hat{x}(T)$ marked roots of a polynomial Chebyshev, which are determined by the formula (10):

$$\hat{x}(T) = -\cos\frac{\Pi(2u-1)}{2n} \tag{10}$$

where u – number of systems,
or specified for tables [12] for $n = 2$ i $u = 1$ $\hat{x}(T) = -0{,}7071$, and for $n = 2$ i $u = 2$ $\hat{x}(T) = 0{,}7071$ in the specified range $\hat{x}(T) \in [-1, 1]$. They correspond to the values of the input quantity requiring real transformation from the actual magnitude $[x_{\min}, x_{\max}]$ to the values belonging to the interval $[-1, 1]$, i.e. the value of standardized (coded) or standardized factor values.

In the case of Chebyshev polynomials, relatives are used:

$$x = 0{,}5[\hat{x}(T)(x_{\max} - x_{\min}) + x_{\min} + x_{\max}] \tag{11}$$

Using the dependency (11) the values of the test plan setting were specified and the results are presented in Table 1.

TABLE 1

The size of the actual elimination plan in the initial sample corresponding to the values used in the trials regulated by surfacing technology

Designation in the initial research plan	**Designation of the actual magnitude**	**Unit of measurement**	**Calculated size**		**Accepted size**		
			–1	**1**	**–1**	**1**	**0**
X1	V_{NAP}	mm/min	124,7	195,4	130	190	160
X2	B	mm	24,39	45,61	25	45	35
X3	Vosc	mm/s	29,1	47,1	29,6	46,6	38,1
X4	P	W	10090	12930	10045	12915	11480
X5	V_d	mm/s	85,4	109,3	88,9	105,8	97,4
X6	L_e	mm	19,39	40,61	20	40	30
X7	l	W/mK	—	—	0,15	4,3	2,15

Power control occurs by regulating the voltage set point source, which results in a change in the voltage across the terminals of the power source. The wire feed speed is regulated independently. On the basis of technological tests the size of the set wire feed was determined.

Values adopted (Table 1) were put in the research plan 2^{k-p} for input quantities 7 and 8 levels with the central plan.

The normalized value $X7$ determined by thermal conductivity was adopted with properties of materials used for heat removal. Individual standardized value [–1, 0, +1] and corresponding actual value [0,15; 2,15; 4,3] respectively, characterize coefficient of thermal conductivity for the low-carbon steel, aluminium and copper.

After determining the input values of polynomial Chebyshev input values array was created for individual experiment plans based on the Experimental Design module Statistic. Table 2 contains the size of standardized plan that has been replaced by the actual relevant parameters in the locations specified on the basis of random number tables. Other technological parameters were determined on the basis of studies of the optimal value of preliminary tests, i.e. the frequency of oscillation $V_{osc} = 2{,}4$ m/min, wire feed speed $V_d = 5{,}8$ m/min, width of amplitude of bead $B = 35$ mm.

TABLE 2

The input quantities encrypted and the corresponding actual size (Fi-dummy variables)

Encrypted size	**X1**	**X2**	**X3**	**X4**	**X5**	**X6**	**X7**
Actual size	V_{NAP}	F_1	F_2	P	F_3	l_e	l

To determine the geometry of bead makro specimen was used, on which the hight of bead Hn and depth of penetration Hw was shown. Fig. 2 shows the importance of the parameters of geometry bead. In publications values Fn (area of cladding) and Fw (area of fusion) are defined to set dilution level (W) according to formula $W = (Fw/(Fn + Fw)) \cdot 100\%$.

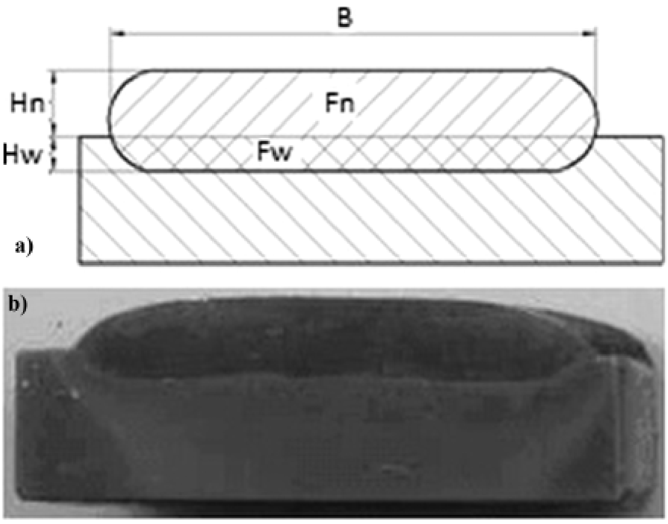

Fig. 2. The size of the weld characteristics (a) and the metallographic section of the clad (b)

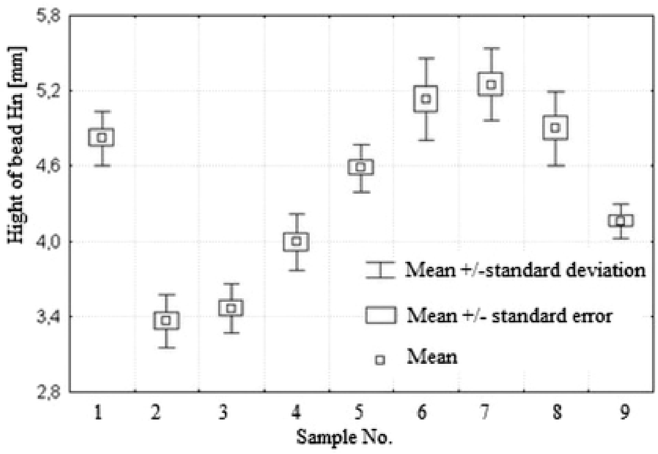

Fig. 3. The standard deviation of the hight of bead measurements *Hn* for test plan.

Table 3 summarizes the results of hight of bead measurements, and Figure 3 shows the results for each test plan experiment.

TABLE 3

Hight of bead measurements *Hn* [mm]

Measurement no.	Sample no.								
	1	2	3	4	5	6	7	8	9
1	4,52	3,16	3,14	3,86	4,45	4,82	5,26	4,59	4,07
2	4,62	3,21	3,24	3,76	4,85	5,02	5,56	4,89	4,17
3	4,72	3,36	3,34	3,86	4,35	5,12	5,76	4,69	4,07
4	4,82	3,46	3,44	4,06	4,75	5,12	5,16	4,59	4,07
5	4,92	3,61	3,54	4,46	4,55	5,12	5,26	4,89	4,47
6	5,02	3,76	3,74	3,96	4,55	5,22	5,16	4,69	4,17
7	5,02	3,16	3,64	3,76	4,45	4,82	5,06	5,19	4,07
8	5,12	3,21	3,64	4,06	4,45	5,92	4,76	5,39	4,07
9	4,62	3,36	3,44	4,16	4,85	5,02	5,26	5,19	4,27
Mean	4,82	3,37	3,46	3,99	4,58	5,13	5,25	4,9	4,16
Standard deviation	0,21	0,21	0,2	0,22	0,19	0,33	0,29	0,29	0,14
Variance	0,05	0,05	0,04	0,05	0,04	0,11	0,08	0,09	0,02
Population	9	9	9	9	9	9	9	9	9
Min variance	4,52	3,16	3,14	3,76	4,35	4,82	4,76	4,59	4,07
Max variance	5,12	3,76	3,74	4,46	4,85	5,92	5,76	5,39	4,47
Range	0,6	0,6	0,6	0,7	0,5	1,1	1	0,8	0,4

To determine the linearity of hight of bead distribution *H* hypothesis H_0; $\overline{x}_{1...8} = \overline{x}_9$ was verified, to contrast with the alternative hypothesis H_1; $\overline{x}_{1...8} \neq \overline{x}_9$, Character test (9) was used. Table 4 summarizes the results of the test.

TABLE 4

The collected statistics describing the value of the hight of bead

Sample no.	Mean	Variance	Population	The calculated value of statistics *t*-Student
1...8	4,44	0,539	72	1,1246
9	4,16	0,019	9	

Assuming a level of significance $\alpha = 0{,}05$ with the number of degrees of freedom $n_1 + n_2 = 81$ critical value statistics *t*-Student: $t_{0{,}05;81} = 2{,}8898$ was specified.

The results allow to infer the distribution of hight of bead *H* linearity and give no reasons for rejecting the hypothesis H_0.

Similarly, as for the height of the bead *Hn*, the measurements of the depth of penetration *Hw* were conducted. Table 5 summarizes the results of the depth of bead measurements, and Figure 4 shows the results for each test plan experiment.

TABLE 5

Depth of bead measurements Hw [mm]

Measurement no	Sample no.								
	1	2	3	4	5	6	7	8	9
1	1,32	2,82	0,84	1,92	1,36	1,23	0,7	1,79	1,34
2	0,48	2,04	0,68	1,67	2,12	1,23	1,37	1,39	1,64
3	1,26	2,03	1,1	1,27	2,26	1,16	0,85	1,52	1,25
4	1,17	1,65	1,08	1,4	2,29	1,39	1,23	1,56	1,6
5	1,73	1,45	1,22	1,53	2,4	1,01	1,29	1,59	1,27
6	0,99	1,36	1,23	1,74	1,9	0,73	0,75	0,89	1,45
Mean	1,16	1,89	1,03	1,59	2,06	1,13	1,03	1,46	1,43
Standard deviation	0,41	0,54	0,22	0,24	0,38	0,23	0,3	0,31	0,17
Variance	0,17	0,29	0,05	0,06	0,15	0,05	0,09	0,09	0,03
Population	6	6	6	6	6	6	6	6	6
Min variance	0,48	1,36	0,68	1,27	1,36	0,73	0,7	0,89	1,25
Max variance	1,73	2,82	1,23	1,92	2,4	1,39	1,37	1,79	1,64
Range	1,25	1,46	0,55	0,65	1,04	0,66	0,67	0,9	0,39

To determine the linearity of the depth of bead measurements *Hw* hypothesis H_0; $\overline{x}_{1...8} = \overline{x}_9$ was verified, to contrast with the alternative hypothesis H_1; $\overline{x}_{1...8} \neq \overline{x}_9$, Character test (9) was used. Table 6 summarizes the results of the test.

Assuming a level of significance $\alpha = 0{,}05$ with the number of degrees of freedom $n_1 + n_2 = 54$ critical value statistics *t*-Student: $t_{0{,}05;54} = 2{,}0081$ was specified.

The results allow to infer the distribution of depth of bead *Hw* linearity and give no reasons for rejecting the hypothesis H_0.

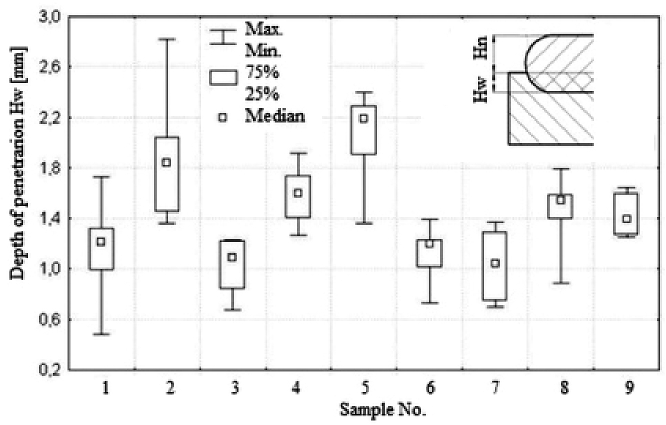

Fig. 4. The standard deviation of the depth of bead measurements Hw for test plan

TABLE 6

The collected statistics describing the depth of bead measurements *Hw*

Sample no.	Mean	Variance	Population	The calculated value of statistics *t*-Student
1...8	1,42	0,243	48	0,0414
9	1,43	0,028	6	

3. Discussion

Based on the analysis of hight of bead measurement *Hn* (Table 3) it is stated that, the average value is in the range from 3,37 to 5,25 mm. The highest value was achieved when measuring the sample number 5, which was made with the following parameter setting (V_{NAP} = 190 mm/min, P = 12915 W, L_e = 40 mm, λ = 0,15 W/mK). The largest scattering of the measurements was observed for samples made according to plan number 6: (V_{NAP} = 190 mm/min, P = 10045 W, L_e = 40 mm, α = 4,3 W/mK), for which the maximum measured hight was observed at rate 5,13 mm.

Analyzing the impact of length parameters of free outlet electrodes and cladding speed on the test factor (Fig. 5) it can be observed that, higher value /*Hn*/ was obtained for the long protruding section of the electrode and lower speed ranges.

Analyzing the impact of the power and thermal conductivity (Fig. 6) the following results can be noticed. The thermal conductivity affects the obtainable of bead at the high power settings source. Attention should be paid to the behavior of the high values in relation to the lower power setting. In this respect, the influence of the thermal conductivity is higher.

Analyzing the impact of thermal conductivity and cladding speed to the test factor such as depth of bead *Hw* (Fig. 7). Lower value *Hw* was obtained for the low thermal conductivity and lower speed ranges and also for higher thermal conductivity and higher speed ranges.

Analyzing the impact of length parameters of free outlet electrodes and the power (Fig. 8), it can be notice, that at high power the source affects the thermal conductivity at obtainable

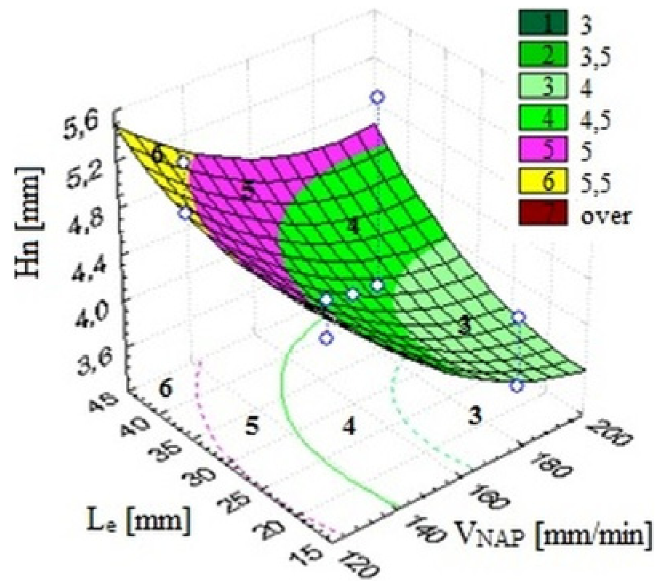

Fig. 5. Impact parameters of free outlet electrode and cladding speed on hight of bead *Hn*

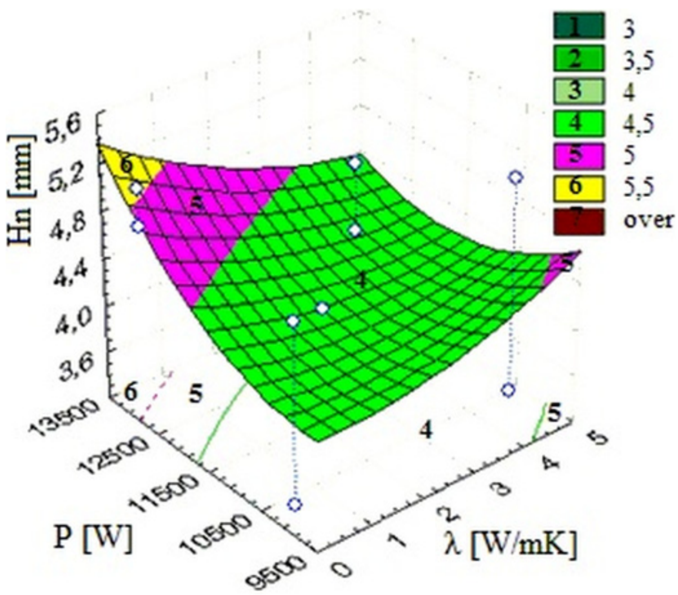

Fig. 6. The effects of setting parameters of the power source and the thermal conductivity of the hight of bead *Hn*

hight of bead. Attention should be paid to high values of the depth of bead *Hw* in relation to the lower length parameters of free outlet electrodes.

In order to develop a mathematical model of the process of surfacing wear-resistant flooring, relationship between the input quantities (independent variables) was examined in the form of technological parameters $X1$, $X4$, $X6$, $X7$ cladding speed respectively V_{NAP} = 130 mm/min, arc power P = 11478 W, length of free outlet wire L_e = 40 mm, thermal conductivity coefficient λ = 3,7 W/mK, and the size of the subsidiary adopted the following general form of regression equation in the form (12).

$$y = B_0 + B_1x_1 + B_2x_2 + B_3x_3 + B_4x_4 \tag{12}$$

whereby: B_i – coefficients of the regression equation.

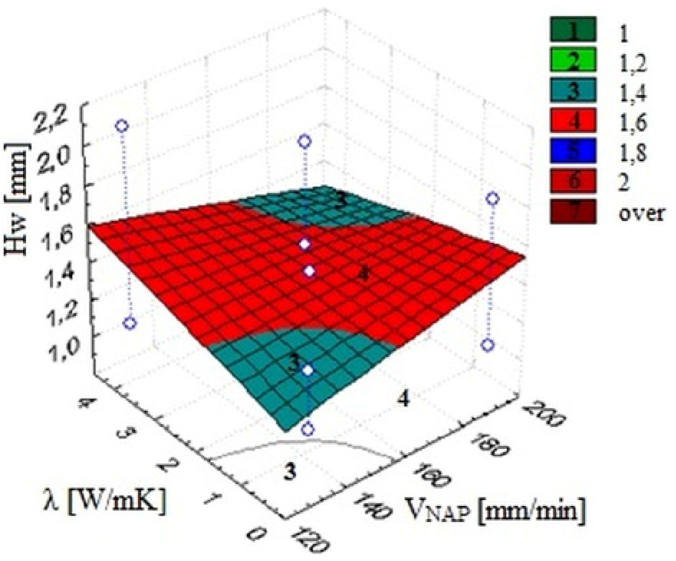

Fig. 7. The effects of setting parameters of the thermal conductivity and cladding speed on the depth of penetration *Hw*

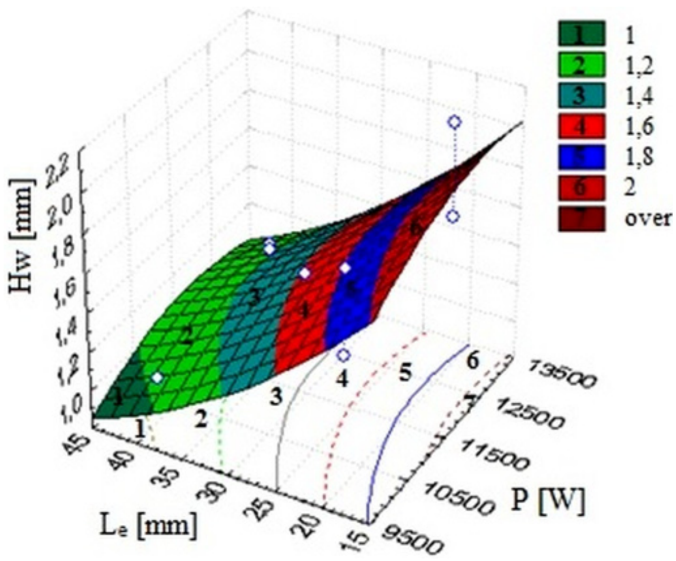

Fig. 8. The effects of setting parameters of the length the projecting portion of the electrode and the power source on the depth of penetration *Hw*

Volumes determined in the equation (12) assigned parameter $X1$ research plan size x_1 regression equation and appropriate for the size of $X4$ – assigned to x_2 and sequentially $X6$-x_3 and $X7$-x_4, then the equation (12) takes the form (13)

$$y = B_0 + B_1 \cdot V_{NAP} + B_2 \cdot P + B_3 \cdot Le + B_4 \cdot \lambda \qquad (13)$$

To determine the regression equation, the input values contained in Table 5 were used. Replacing the actual values with encoded amounts at the levels of [–1, +1], and the value of the output in the form of mean values of the analyzed coefficient i.e. hight of bead *Hn* (Table 3), and depth of penetration *Hw* (Table 5) was defined.

To determine the coefficients of the regression equation statistics dependences (2) and (3) were used. Dependency (4) to determine the variance of the experiment error. Dependency (5), to determine the standard deviation and formula (6) to determine the significance of the influence of the analyzed factors on the level of significance $\alpha = 0,05$ to 7 degrees of freedom. The collected coefficients and statistics are included in Table 7.

Considering the values of the coefficients the regression equation may be determined at a significance level $\alpha = 0,05$. Form of the equation for the analyzed agent is as follows:

– for hight of clad:

$$Hn = 4,438 + 0,45 \cdot V_{NAP} + 0,193 \cdot L_e \qquad (14)$$

– for depth of penetration:

$$Hw = 1,419 + 0,066 \cdot L_e \qquad (15)$$

4. Conclusion

Applying the plan of experiment allows to precisely define the impact of factors on the final properties. Analyzing the impact of each welding process parameters such as welding speed, power setting source, the length of the projecting portion of the electrode and method of heat removal determined by the thermal conductivity of the material lining the table, it can be concluded that the influence of the examined factors on the parameters of geometry of the layers obtained are as follows:

- Length of protruding section is of particular importance to depth of bead. The higher setting the lower depth of bead.
- Increasing the length of protruding section allows to develop the layer with the lowest depth of bead.
- Impact of speed surfacing is strongly correlated to the thermal conductivity.
- Character of geometry changes depend on material used to conduct the term.
- When using steel to conduct the term, increase in speed of welding causes the increase of depth of bead.
- When using copper to conduct the term, increase in speed of welding causes the decrease of depth of bead.
- Setting the source power at a low value allows to use the parameters of the heat removal for plates made of steel, aluminium or copper. This can be seen especially for low-power parameters source, where increase of high of bead, depends on the material used for heat removal in cooling

TABLE 7

Coefficients of the regression equations and statistics

Coefficients	B_0	B_1	B_2	B_3	B_4	a_0	a_1	a_2	a_3	a_4	S_n^2	S_i^2	S_i	$t_{0,05;7}$	$t_{0,05;7}S_i$
Hn	4,438	–0,45	–0,118	0,193	–0,08	2,219	–0,225	–0,059	0,096	–0,04	0,111	0,009	0,096	2,365	0,228
Hw	1,419	–0,009	0,009	0,066	–0,001	0,709	–0,004	0,004	0,033	–0,001	0,002	0	0,013	2,365	0,03

process. High values were obtained especially for intensive cooling while using cooper plates. Increase in power settings causes decrease of the influence of the applied heat reception. It can be concluded that the heat capacity of the cooling plates is not sufficient (10 mm) and their thickness in case of higher setting of the power source could be increased.

REFERENCES

[1] T. Chmielewski, K. Kudła, M. Węglowski, Institute of Welding Bulletin **58** (5), 193-197 (2014) (in Polish).

[2] R. Bęczkowski, M.Gucwa, Archives of Foundry Engineering **16** (4), 23-28 (2016).

[3] R. Bęczkowski, M. Gucwa, J. Wróbel, A. Kulawik, AIP CONF PROC 1738, 480095 (2016); DOI: 10.1063/1.4952331.

[4] J. Górka, M. Adamiak, E. Darda, Welding Technology Review **83** (7), 31-35 (2011) (in Polish).

[5] Gucwa, R. Bęczkowski, Welding Technology Review **83** (10), 77-80 (2011) (in Polish).

[6] P.F. Mendez, N. Barnes, K. Bell, S.D. Borle, S.S. Gajapathi, S.D. Guest, H. Izadi, A.K. Gol, G. Wood, Journal of Manufacturing Processes **16**, 4-25 (2014).

[7] J. Niagaj, Welding Technology Review (10), 67-72 (2011).

[8] R. Bęczkowski, METABK **56** (1-2), 59-62 (2017).

[9] L. Kukiełka, Podstawy badań inżynierskich, 2002 PWN, Warszawa (in Polish).

[10] M. Korzyński, Metodyka eksperymentu, 2013 WNT, Warszawa (in Polish).

[11] D. Jańczewski, C. Różycki, L. Synoradzki, Projektowanie procesów technologicznych, 2010 Oficyna Wydawnicza PW, Warszawa (in Polish).

[12] Z. Polański, Planowanie doświadczeń w technice, 1984 PWN, Warszawa (in Polish).

[13] S. Buytoz, M.M. Yildirim, Archives of Foundry Engineering **10** (1), 279-286 (2010).

[14] A. Zikin, I. Hussainova, C. Katsich, E. Badisch, C. Tomastik, Surf. Coat. Tech. **206**, 4270-4278 (2012).

[15] M. Bonek, Arch. Metall. Mater. **61** (2), 719-724 (2016).

[16] M.B. Ashok Kumar, N. Murugan, I. Dinaharan, Trans. Nonferrous Met. Soc. China **24** (2014), DOI: 10.1016/S1003-6326(14)63410-5.

[17] J. Szajnar, A. Walasek, C. Baron, Arch Metall Mater **58** (3) 931-936 (2013); DOI: 10.2478/amm-2013-0104.

[18] N. Bajić, D. Bajić, D. Veljić, M. Rakin, Z. Janjušević, METABK **53** (3), 361-364 (2014).

[19] I. Pernis, J. Kasala, D. Žabecká, METABK **52** (3), 352-354 (2013).

[20] V. Shevelya, W. Orłowicz, A. Trytek, V. Kirilkov, Archives of Foundry Engineering **10** (1), 273-278 (2010).

[21] A.W. Orłowicz , M. Mróz, M. Tupaj, J. Betlej, F. Páoszaj, Archives of Foundry Engineering **9** (2), 113-118 (2009).